



# NAVAL POSTGRADUATE SCHOOL

MONTEREY, CALIFORNIA

## THESIS

**FIELD OBSERVATION OF SETUP**

by

Sean P. Yemm

June 2004

Thesis Advisor:  
Second Reader:

Edward Thornton  
Timothy Stanton

**Approved for public release; distribution is unlimited.**

THIS PAGE INTENTIONALLY LEFT BLANK

<b>REPORT DOCUMENTATION PAGE</b>			<i>Form Approved OMB No. 0704-0188</i>	
Public reporting burden for this collection of information is estimated to average 1 hour per response, including the time for reviewing instruction, searching existing data sources, gathering and maintaining the data needed, and completing and reviewing the collection of information. Send comments regarding this burden estimate or any other aspect of this collection of information, including suggestions for reducing this burden, to Washington headquarters Services, Directorate for Information Operations and Reports, 1215 Jefferson Davis Highway, Suite 1204, Arlington, VA 22202-4302, and to the Office of Management and Budget, Paperwork Reduction Project (0704-0188) Washington DC 20503.				
<b>1. AGENCY USE ONLY (Leave blank)</b>		<b>2. REPORT DATE</b> June 2004	<b>3. REPORT TYPE AND DATES COVERED</b> Master's Thesis	
<b>4. TITLE AND SUBTITLE:</b> Title (Mix case letters) Field Observation of Setup			<b>5. FUNDING NUMBERS</b>	
<b>6. AUTHOR(S)</b> Yemm, Sean P.				
<b>7. PERFORMING ORGANIZATION NAME(S) AND ADDRESS(ES)</b> Naval Postgraduate School Monterey, CA 93943-5000			<b>8. PERFORMING ORGANIZATION REPORT NUMBER</b>	
<b>9. SPONSORING / MONITORING AGENCY NAME(S) AND ADDRESS(ES)</b> N/A			<b>10. SPONSORING / MONITORING AGENCY REPORT NUMBER</b>	
<b>11. SUPPLEMENTARY NOTES</b> The views expressed in this thesis are those of the author and do not reflect the official policy or position of the Department of Defense or the U.S. Government.				
<b>12a. DISTRIBUTION / AVAILABILITY STATEMENT</b> Approved for public release; distribution is unlimited			<b>12b. DISTRIBUTION CODE</b>	
<b>13. ABSTRACT (maximum 200 words)</b>  Setup is defined as the superelevation of mean water surface within the surfzone and is caused by the reduction in wave momentum shoreward of the breaking point and compensating positive pressure gradient. Data were acquired north of Scripps Canyon on a gently sloping section of beach, which was homogenous in along-shore morphology, during the Nearshore Canyon Experiment, 2004. Pressure sensors were deployed both above and below the bed. Wave heights and radiation stress (wave-induced momentum) were calculated using linear theory transfer functions. Wave heights measured using pressure sensors in the water column had a positive bias compared with the buried pressure sensors, which it is presumed due to the Bernoulli effect of flow past the orifices. Predicted setup based on numerically solving the cross-momentum equation forced with the measured radiation stresses underestimates the observed setup by 40 percent in the mean. This is consistent with previous studies.  .				
<b>14. SUBJECT TERMS</b> Oceanography, Nearshore, Setup, Radiation Stress, NCEX			<b>15. NUMBER OF PAGES</b> 45	
			<b>16. PRICE CODE</b>	
<b>17. SECURITY CLASSIFICATION OF REPORT</b> Unclassified	<b>18. SECURITY CLASSIFICATION OF THIS PAGE</b> Unclassified	<b>19. SECURITY CLASSIFICATION OF ABSTRACT</b> Unclassified	<b>20. LIMITATION OF ABSTRACT</b> UL	

THIS PAGE INTENTIONALLY LEFT BLANK

**Approved for public release; distribution is unlimited.**

**FIELD OBSERVATION OF SETUP**

Sean P. Yemm  
Lieutenant, United States Navy  
B.S., United States Naval Academy, 1997

Submitted in partial fulfillment of the  
requirements for the degree of

**MASTER OF SCIENCE IN METEOROLOGY AND PHYSICAL  
OCEANOGRAPHY**

from the

**NAVAL POSTGRADUATE SCHOOL  
June 2004**

Author: Sean P. Yemm

Approved by: Edward B. Thornton  
Thesis Advisor

Timothy Stanton  
Second Reader

Mary Batteen  
Chairman, Department of Oceanography

THIS PAGE INTENTIONALLY LEFT BLANK

## **ABSTRACT**

Setup is defined as the superelevation of mean water surface within the surfzone and is caused by the reduction in wave momentum shoreward of the breaking point and compensating positive pressure gradient. Data were acquired north of Scripps Canyon on a gently sloping section of beach, which was homogenous in along-shore morphology, during the Nearshore Canyon Experiment, 2004. Pressure sensors were deployed both above and below the bed. Wave heights and radiation stress (wave-induced momentum) were calculated using linear theory transfer functions. Wave heights measured using pressure sensors in the water column had a positive bias of about 5 percent compared with the buried pressure sensors, which is presumed due to the Bernoulli effect of flow past the orifices. Predicted setup based on numerically solving the cross-momentum equation forced with the measured radiation stresses underestimates the observed setup by 40 percent in the mean. This is consistent with previous studies.

THIS PAGE INTENTIONALLY LEFT BLANK

## TABLE OF CONTENTS

<b>I.</b>	<b>INTRODUCTION.....</b>	<b>1</b>
<b>II.</b>	<b>THEORY .....</b>	<b>3</b>
<b>III.</b>	<b>EXPERIMENT .....</b>	<b>5</b>
<b>IV.</b>	<b>DATA ANALYSIS.....</b>	<b>7</b>
	<b>A. OBSERVED SETUP/DOWN.....</b>	<b>7</b>
	<b>B. WAVE HEIGHTS.....</b>	<b>7</b>
	<b>C. RADIATION STRESS .....</b>	<b>8</b>
	<b>D. GRADIENT BALANCE .....</b>	<b>9</b>
	<b>E. THEORETICAL SETUP.....</b>	<b>9</b>
<b>V.</b>	<b>RESULTS .....</b>	<b>11</b>
	<b>A. WAVE HEIGHTS.....</b>	<b>11</b>
	<b>B. RADIATION STRESS .....</b>	<b>13</b>
	<b>C. GRADIENT BALANCE .....</b>	<b>14</b>
	<b>D. OBSERVED VS. THEORETICAL SETUP.....</b>	<b>15</b>
<b>VI.</b>	<b>DISCUSSION .....</b>	<b>17</b>
<b>VII.</b>	<b>CONCLUSIONS .....</b>	<b>19</b>
	<b>LIST OF REFERENCES.....</b>	<b>29</b>
	<b>INITIAL DISTRIBUTION LIST .....</b>	<b>33</b>

THIS PAGE INTENTIONALLY LEFT BLANK

## LIST OF FIGURES

Figure 1.	Observed wave height, period and direction over the course of the experiment.....21
Figure 2.	Location of Paroscientific and Kulite pressure transducers relative to the bed and mean sea level. Open circles beneath the profile represent Paroscientific sensors. Open diamonds signify Kulite sensors. Instruments are numbered from the closest onshore to the furthest off.....22
Figure 3.	Wave heights (in cm) generated by colocated Paroscientific and Kulite pressure transducers.....23
Figure 4.	Wave heights (in cm) generated by colocated Paroscientific pressure transducer and Marsh McBirney electromagnetic current velocimeter.....24
Figure 5.	Wave heights (in cm) generated by colocated Marsh McBirney electromagnetic current velocimeter and Kulite pressure transducer.....25
Figure 6.	Radiation Stress generated by colocated Paroscientific pressure transducer and Marsh McBirney electromagnetic current velocimeter. Radiation stresses plotted on the abscissa were derived from pressure data alone. Radiation stresses plotted in the ordinate were derived from pressure and velocity data.....26
Figure 7.	Calculated shoreward changes in radiation stress vs. surface elevation gradients between Instrument 7 and subsequent inshore instruments. The radiation stress gradient has been divided by $-\rho g(h + \eta)$ for comparison.....27
Figure 8.	Observed superelevation of mean water level plotted against the theoretical setup. Instrument 5 is excluded.....28

THIS PAGE INTENTIONALLY LEFT BLANK

## I. INTRODUCTION

Setup is qualitatively defined as the wave induced superelevation of mean water surface above the still water level shoreward of the breakpoint. As waves approach the shore and shoal, the wave energy momentum flux increases as depth decreases, resulting in a compensating depression in the mean surface level, or setdown. Further onshore, waves break and undergo an immediate reduction in height and energy. The shoreward dissipation of energy and accompanying decrease in momentum flux, referred here after as radiation stress, is balanced by a rise in pressure gradient, manifested in a steady, shoreward increase in surface elevation. This upward slope in surface elevation is setup.

Beach morphology and circulation in the nearshore dictate research interest in setup. Wave-induced higher mean sea levels can yield greater erosion and flooding further inland. In extreme cases such as storm-built, towering waves, potentially significant property damage and loss of life could be incurred. Longshore gradients of setup due to differences in offshore wave energy generate longshore flow within the surfzone. Consequently, understanding of setup is essential to developing predicative models for nearshore circulation.

Wave setup has been a topic of interest with researchers since a hurricane struck the East Coast of the United States in 1938, producing an escalation in the mean water surface in exposed areas beyond the increase due to storm-surge in sheltered areas. The increase was hypothetically attributed to breaking waves. Subsequent laboratory observations confirmed the existence of setup and its relationship to the incoming wave field [see for example *Savage, 1957; Fairchild, 1958; Saville, 1961; Bowen et al., 1968*]. Qualitative descriptions of wave-generated setup were corroborated and complemented by theoretical analysis, which related shoreward momentum flux to pressure gradient [*Longuet-Higgins and Stewart, 1963*] and detailed quantitative observations from laboratory models [*Bowen et al., 1968; Battjes, 1974; Battjes and Stive, 1985; Haller et al., 2002; Svendsen, 1984; Diegaard et al., 1991; Schaffer et al., 1993; Stive and Wind, 1982; Reniers and Battjes, 1997*]. Setup in the laboratory can be easily measured using manometers with orifices mounted flush to the bed.

In addition to measurements in the laboratory, observations have been obtained in the field. Field studies have been conducted over near planar beaches [*Guza and Thornton, 1981; Nielsen, 1988; King et al., 1990*], and over barred beaches [*Lentz and Raubenheimer, 1999; Raubenheimer et al, 2001*]. A variety of techniques have been employed to measure setup. Measuring setup in the field requires accurate and stable sensors. *Guza and Thornton [1981]* measured maximum set with a resistance wire stretched across the cross-shore swash. *Nielsen [1988]* used manometer tubes referenced to the offshore and measured by a ruler averaged by eye; this makes these measurements noisy. *King et al., [1990]* used accurate Paroscientific sensors, which unfortunately were installed up in the water column. A Bernoulli effect contaminates pressure sensors in the water column as current passes over the pressure orifices. The Bernoulli effect can be comparable or greater than setup values. For this reason *Raubenheimer et al, [2001]* buried their Paroscientific pressure sensors to obtain accurate results. In the experiment described below, the approach by *Raubenheimer et al, [2001]* is followed and buried Paroscientific pressure sensors are used to measure setup/down.

## II. THEORY

As waves shoal, wave-induced momentum (termed radiation stress) increases as the wave height increases with decreasing depth. However, once the waves start to break in the surfzone, the radiation stress decreases. Neglecting viscous forces, these changes in radiation stress are balanced by changes in hydrostatic pressure forces resulting in set-down and set-up of the mean sea level, given by (*Longuet-Higgins and Stewart, 1962*):

$$\frac{\partial S_{xx}}{\partial x} = -\rho g (h + \eta) \frac{\partial \eta}{\partial x}, \quad (1)$$

where  $S_{xx}$  is the radiation stress,  $\rho$  is density,  $g$  is gravitational acceleration,  $h$  is the water depth from still water level to bed, and  $\eta$  is mean surface elevation relative to still water level. Coordinates  $x$  and  $z$  are aligned cross-shore and vertical, oriented positive onshore and upward from still water level. Bottom contours are assumed straight and parallel so that changes in alongshore direction  $y$ , are neglected.

The x-component of radiation stress is given by (*Phillips, 1977*)

$$S_{xx} = \overline{\int_{-h}^{\eta} \rho (u^2 + p) dz}, \quad (2)$$

where  $u$  is wave-induced velocity and the overbar indicates time average. The wave induced pressure is given by

$$p(z) = \rho g (\eta' - z) + \frac{\partial}{\partial t} \int_z^{\eta} \rho \omega dz + \frac{\partial}{\partial x} \int_z^{\eta} \rho u \omega dz - \rho \omega^2. \quad (3)$$

Applying linear wave theory to second order, *Longuet-Higgins and Stewart [1962]* obtained:

$$S_{xx} = E \left( \frac{C_g \cos^2 \alpha}{C} \right) + E \left( \frac{2C_g}{C} - 1 \right), \quad (4)$$

where  $E$  is the wave energy,  $C_g$  and  $C$  are the group and phase speed,  $\alpha$  is the wave direction. In shallow water with waves assumed to be normal to the beach, the radiation stress reduces to

$$S_{xx}(x) = \frac{3}{2} E \quad (5)$$

For a Rayleigh distribution of wave heights,  $E$  is given by:

$$E = \frac{1}{8} \rho g H_{rms}^2, \quad (6)$$

where  $H_{rms}$  is the root-mean-square wave height for random waves (*Battjes and Janssen, 1978*). Although linear wave theory is generally not valid inside the surfzone, *Guza and Thornton [1981]* found local estimates to be reasonably accurate. For narrow band waves,  $H_{rms}$  is approximated by

$$H_{rms} = 2\sqrt{2} \sigma_{\eta}, \quad (7)$$

where  $\sigma_{\eta}$  is the standard deviation of the surface elevation.

### III. EXPERIMENT

The Nearshore Canyon Experiment was conducted on Black's Beach onshore of Scripps Canyon, approximately 2.5km north of the University of San Diego's Scripps Institution of Oceanography (SIO) Pier, San Diego, California in the autumn of 2003. Black's Beach is characterized by moderately sorted, fine grain sand (mean diameter of 0.1mm), a gentle, near planar ( $\sim 1:50$ ), slope, and a homogenous longshore bathymetry. Significant wave heights were typically between 0.5 and 0.7m, peaking at 1.5m the evening of yearday 320 (Figure 1). The lowest wave day during the experiment was on yearday 319, during which significant wave height were less than 0.5m. Hourly peak wave periods varied between five and twelve seconds during the experiment. Waves propagated along a line perpendicular to the shore, from roughly  $270^\circ$ , with little variation. Winds during the experiment were light, never rising above 6m/s, and varying from West (onshore) during the day to East (offshore) at night, characteristic of a diurnal sea breeze.

The cross-shore array of instrumentation (Figure 2) was installed to explore the interactions between wave breaking, nearshore circulation and beach morphology. Cross-shore variations of wave height, radiation stress and set-up/down were observed using eight pressure-velocity (PUV) instruments arranged along a transect normal to the shoreline and spaced roughly 25m apart. Data from the PUVs were acquired near continuously from yearday 305 to yearday 323. Bathymetric profiles were obtained by wheeling a dolly with attached kinematic differential GPS into the surf, recording data in latitude, longitude and altitude relative to mean sea level. Profile and sensor locations are depicted in Figure 2, relative to MSL.

Each of the seven inshore PUVs, instruments 1 through 7 in Figure 2, were equipped with a Paroscientific Digiquartz Depth Sensor to measure setup/setdown. The sensors were buried approximately 80cm below the sand bed (location shown in Figure 2) so that they would not be exposed to currents that can induce a Bernoulli pressure. The sensors have a depth range of 0 to 10 meters. The manufacturers accuracy is  $\pm 2\text{mm}$  (0.02% of full scale), including repeatability, hysteresis, and temperature sensitivity. The Paroscientific pressure data were sampled at 1Hz. The sensors were pre- and post-

calibrated to assess potential errors. Stability tests for the Paroscientific sensors were conducted by keeping them in a constant temperature and pressure bath for 3-4 days to verify their stability. After correction for atmospheric pressure, the sensor depth readings remained within  $\pm 3$ mm rms of the measured water depth throughout all tests. Calibrations were obtained by maintaining constant temperature as the pressure was raised to 2.5m of water and then lowered gradually at 10cm increments. Temperature calibration was performed for the range of temperature 8-16°C, while maintaining constant pressure. Corrected pressure readings varied by  $\pm 1$ cm rms or less during these tests.

Kulite XTM-190-50A pressure sensors were located on instruments 3 through 8, the six PUVs furthest offshore, roughly 50cm above the bed, as shown in Figure 1. The sensors have a range of 0-50psia and an accuracy of .2% of full scale. Marsh-McBirney Model 512, Electromagnetic Water Current Meters were colocated on the PUV 28cm below the Kulite pressure sensors and about 15cm above the bed. The current velocities and pressure from the Kulite sensors were sampled at 14Hz.

Barometric pressure was measured using atmospheric pressure sensors located at the end of Scripps Pier. Atmospheric pressure was recorded in millibars at a rate of once per hour. The atmospheric pressure is subtracted off the absolute pressure reading to obtain head of water.

## IV. DATA ANALYSIS

### A. OBSERVED SETUP/DOWN

The pressure data were converted from millibar to seawater pressure head in centimeters by subtracting the barotropic pressure and multiplying the difference by a conversion factor. For data quality control, data outside 3 standard deviations of the daily mean were considered erroneous and not included in the average, and small data gaps in time were interpolated. Invalid data, recorded by exposed sensors during periods of low tidal height were likewise excised from the analyzed data set. Hourly mean pressure from yearday 305 to 319 were used as measures of setup/down.

It is not possible to survey the elevation of submerged instrument mounting pipes to the necessary accuracy to determine setup/down. Therefore, all sensors were leveled on the lowest wave day ( $H_{\text{rms}} = 0.2\text{m}$ ), yearday 319 at high tide, when it was assumed that the mean sea level was flat. Surface elevation relative to Mean Sea Level (MSL) was determined by subtracting each instrument's offset from the hourly mean pressure. Instrument offset was subtracted from the mean hourly instrument pressure. Following the removal of instrument offset, surface elevation from the furthest offshore instrument (see Figure 1) was subtracted from the remaining inshore instruments to remove tidal fluctuation with the assumption that there is no setup/down at the furthest offshore sensor.

### B. WAVE HEIGHTS

$H_{\text{rms}}$  wave heights were calculated using (7), where the variance of the surface elevation is obtained by summing the spectrum over the sea-swell band of frequencies (0.05-0.25Hz). The surface elevation spectra were calculated in three ways from pressure and current velocity using linear theory spectral transformations,  $G_{\eta}(f) = |H_{p,u}(f)|^2 G_{p,u}(f)$ . Averaged spectra were calculated using one-hour records divided into 30 two-minute sub-intervals to give 60 degrees of freedom. A Hanning window was applied to the time series data prior to spectra calculations.

The transfer function used for the kulite pressure sensors, located above the bed, is

$$H_p(f) = \frac{\cosh(kh)}{\cosh(kz)}, \quad (8)$$

where  $k$  is the wave number,  $h$  is the hourly averaged water depth, and  $z$  is the elevation of the sensor above the bed. The transfer function used to convert current velocity is:

$$H_u(f) = \frac{C}{g} \left[ \frac{\cosh(kh)}{\cosh(kz)} \right], \quad (9)$$

The transfer function for the buried parascientific sensors is [Raubenheimer *et al* (1998)]:

$$H_p(f) = e^{kz} \cosh(kh), \quad (10)$$

where  $z$  is the instrument depth below the bed ( $z$  positive upward from the bed).

### C. RADIATION STRESS

Radiation stresses are similarly calculated using linear theory transfer functions to solve (2) locally using two approaches. The first approach is to transform measured horizontal velocity and pressure spectra to calculate (2) using (3) to second order,

$$S_{xx}(f) = |H_u(f)|^2 G_u(f) + |H_p(f)|^2 G_\eta(f) \quad (11)$$

where  $G_u(f)$  and  $G_\eta(f)$  are the horizontal velocity and surface elevation spectra,

$$|H_u(f)|^2 = \frac{\rho c^2}{g} \left[ \frac{\cosh^2(kh)}{\cosh^2(kz)} \right], \quad (12)$$

and

$$|H_p(f)|^2 = \frac{\rho g}{2} \left[ \frac{2kh}{\sinh(2kh)} \right]. \quad (13)$$

The second approach is to use the pressure to approximate the horizontal velocity in (2) so that  $S_{xx}(f)$  is based on transforming the pressure spectrum alone,

$$S_{xx}(f) = |H_p(f)|^2 G_\eta(f) \quad (14)$$

where

$$|H_p(f)|^2 = \frac{\rho g}{2} \left\{ \cos^2 \alpha \left[ 1 + \frac{2kh}{\sinh(2kh)} \right] + \frac{2kh}{\sinh(2kh)} \right\}, \quad (15)$$

and  $\alpha$  is the mean wave direction relative to shore normal.

### D. GRADIENT BALANCE

The change in surface elevation was determined by subtracting setup at Instrument 7 from setup at subsequent inshore instruments. The shoreward change in radiation stress was similarly determined by subtracting the radiation stress at Instrument 7 from radiation stress at the six subsequent inshore instruments. Radiation stress values were calculated using only the Paroscientific pressure (14). The change in radiation stress was then divided by seawater density, gravitational acceleration, and total mean depth between instruments for comparison with change in setup to evaluate the balance in (1).

#### **E. THEORETICAL SETUP**

Measured setup is compared with theoretical setup. Theoretical mean surface elevation was calculated by numerically solving (1) by iteration at 1m intervals along a cross-shore transect to the beach. The mean sea level is initially assumed level at Instrument 7. The measured radiation stresses at the instruments are linearly interpolated to the 1m steps as forcing for (1). Theoretical setup located at points along the cross-shore transect matching instrument positions were compared with that instrument's corresponding observed setup.

THIS PAGE INTENTIONALLY LEFT BLANK

## V. RESULTS

### A. WAVE HEIGHTS

Wave heights derived from Paroscientific and Kulite recorded pressures and from Marsh-McBirney recorded cross- and along-shore current velocities compare well. The wave heights derived at each instrument location are compared to examine transfer functions. Linear regression slope, offset and correlation coefficient are determined to ascertain the agreement between the sensors being compared.

#### 1. Paroscientific vs. Kulite $H_{rms}$

$H_{rms}$  calculated using data from colocated Paroscientific and Kulite pressure data appears to be well correlated (Figure 3). Wave Heights less than 20cm are not considered as these generally occur at low tide inside the surf zone when the Kulite sensors often come out of the water. All wave heights are plotted in Figure 3 for reference, but only  $H_{rms} > 20\text{cm}$  are considered in the regression analysis. Linear regression slopes are close to one and the offsets show a slight positive bias (Table 1).

The exception is Instrument 5, which has a linear regression slope of 0.63, an offset of 11.69 and a correlation coefficient of 0.71. Pressure data recorded by the Paroscientific sensor located on Instrument 5 tended to be greater than that recorded by its immediate neighbors, on Instruments 4 and 6, for the duration of the experiment. The poor agreement between Paroscientific and Kulite derived  $H_{rms}$  at Instrument 5 is believed to be due to poor pressure data from the Paroscientific sensor.

	Instrument					
	3	4	5	6	7	Mean
Slope	0.88	0.92	0.63	1.05	0.97	0.89
Offset	2.19	-0.11	11.69	5.17	4.11	4.61
Correlation Coefficient	0.87	0.95	0.71	0.91	0.94	0.87

**Table 1.** Linear regression slope, offset and correlation coefficient for  $H_{rms}$  greater than 20cm generated by colocated Paroscientific and Kulite pressure transducers. Offsets are in (cm).

## 2. Paroscientific vs. Current Velocity $H_{rms}$

Wave heights obtained from colocated Paroscientific pressure transducers and Marsh McBirney current velocimeters, shown in Figure 4, also compare well. Once again,  $H_{rms}$  values less than 20cm are not considered in the regression analysis. Results of linear regression analysis (Table 2) show good overall agreement.

Results confirm the previously mentioned problem with Instrument 5. Therefore Instrument 5 will not be used in the setup comparisons. Also, a surprisingly low correlation coefficient of 0.69 is found for Instrument 3. Since Instrument 3 is the closest inshore instrument with a current velocimeter, it is likely that some of the velocity data recorded while the tide was receding or increasing have been retained, contaminating the  $H_{rms}$  estimates.

	Instrument					
	3	4	5	6	7	Mean
<b>Slope</b>	1.00	1.04	0.66	0.98	0.92	0.92
<b>Offset</b>	5.01	0.59	18.46	9.45	5.18	7.74
<b>Correlation Coefficient</b>	0.69	0.88	0.63	0.90	0.86	0.79

**Table 2.** Linear regression slope, offset and correlation coefficient for  $H_{rms}$  greater than 20cm generated by colocated Paroscientific pressure transducer and Marsh McBirney electromagnetic current velocity meter.

## 3. Current Velocity vs. Kulite $H_{rms}$

Comparison of wave heights from colocated Marsh McBirney current velocimeters and Kulite pressure transducers (Figure 5) indicate good agreement, but not as good as when compared with the Paroscientific sensor. It is interesting to note that below 20cm the velocity generated  $H_{rms}$  is higher than that of the Kulite sensor. This can be attributed to the difference in vertical position of the two sensors. Since the Kulite sensor is 28cm higher on the PUV, it is out of the water for longer periods time, and experiences greater influence from advancing and retreating tide.

Regression analysis for this set of wave heights (Table 3) tends to validate doubts about specific sensors already discussed. Judging by the correlation coefficient and linear regression slope of 0.90 and 0.88 respectively, the problems with Instrument 5 appear to be specific to the Paroscientific sensor. Relatively low correlation coefficient of 0.72 and slope of .62 indicate that problems with instrument 3, noted in the Paroscientific vs. current velocity discussion, are particular to that velocimeter. Data and derived values from these sensors should be treated with suspicion.

	Instrument					
	3	4	5	6	7	Mean
Slope	0.62	0.78	0.88	1.03	0.98	0.86
Offset	5.53	2.54	-3.12	-2.96	2.26	0.85
Correlation Coefficient	0.72	0.85	0.90	0.93	0.94	0.87

**Table 3.** Linear regression slope, offset and correlation coefficient for Hrms greater than 20cm generated by colocated Marsh McBirney electromagnetic current velocity meter and Kulite pressure transducer.

## B. RADIATION STRESS

Radiation stresses calculated using (11) and (14) are compared to verify agreement and accuracy (Figure 6). Graphic representation and tabular statistics (Table 4) exhibit agreement in the two computing methods. Even Instrument 5 correlates well, though relatively lower with a correlation coefficient of 0.89. High mean correlation coefficient of 0.93 and mean slope of 1.02 signify good agreement between methods. In

	Instrument					
	3	4	5	6	7	Mean
Slope	0.95	1.04	0.94	1.17	0.98	1.02
Offset	3.82	1.61	69.50	42.37	32.38	29.93
Correlation Coefficient	0.95	0.95	0.89	0.95	0.92	0.93

**Table 4.** Linear regression slope, offset and correlation coefficient for Sxx generated by pressure data and combined velocity and pressure data.

the following, Paroscientific pressure data will be used to calculate radiation stresses for setup/down calculations.

### C. GRADIENT BALANCE

The observed mean shoreward surface elevation gradient is compared with the radiation stress gradient in Figure 7 and Table 5 showing considerable scatter. Gradients between Instruments 3 and 7 and between Instruments 4 and 7 compare well, while gradients between Instruments 1 and 7, 2 and 7, and Instruments 6 and 7 are low.

Poor agreement between gradients can be attributed to bad, erroneous or conflicting data. The quality of data from the Paroscientific pressure transducer located on Instrument 5 is well documented. The great amounts of data, removed from consideration due to tidal fluctuation from the Paroscientific sensor located on PUV 1, accounts for the extremely low correlation coefficient of 0.09 between gradients. The same can be said for Instrument 2, which also had substantial amounts of data removed at low tide, though less than Instrument 1. The difference in gradients between Instruments 6 and 7 is due to setup and setdown, occurring in the same space but alternating in time with tidal modulation, that is not resolved by the calculated radiation stress. The horizontal distance between Instruments 6 and 7 lacks the refinement necessary to resolve the increase in radiation stress due to shoaling and subsequent decrease in radiation stress due to breaking.

	Instrument					
	1-7	2-7	3-7	4-7	6-7	Mean
<b>Slope</b>	0.30	0.93	1.02	1.17	0.27	1.14
<b>Offset</b>	-0.03	0.00	0.00	-0.01	-0.01	-0.01
<b>Correlation Coefficient</b>	0.09	0.55	0.78	0.82	0.37	0.55

**Table 5.** Linear regression slope, offset and correlation coefficient for  $-\partial S_{xx}/\rho g(h+\eta)$  vs.  $\partial\eta$ .

#### D. OBSERVED VS. THEORETICAL SETUP

Observed and theoretical setup are compared showing considerable scatter (Figure 8), summarized in Table 6. Theoretical setup values are calculated by

numerically solving  $\eta_{i+1} = \eta_i - \frac{S_{xx_{i+1}} - S_{xx_i}}{\rho g \left[ h + \left( \frac{\eta_i + \eta_{i+1}}{2} \right) \right]}$ . The mean regression slope of 0.4

indicates theory underestimates the observations. Setup values at Instruments 1 are questionable as described above.

Instruments 3 and 4 have higher correlation coefficients, but low regression slopes. Theoretical setup is lower than the corresponding observed setup by 61% for Instrument 3 and 66% for Instrument 4. *Raubenheimer et al [2001]* noted that in depths less than 2m, theory tends to underestimate setup by ~55%. Regression slopes of 0.39 and 0.34 for Instruments 3 and 4 respectively are low but consistent with that analysis.

Lack of correlation between theoretical and observed setup at Instrument 6 is caused by setdown. The method used to numerically iterate theoretical setup employs radiation stress calculated from observed data. Coarse resolution between Instruments 6 and 7 produces radiation stress that fails to account for setdown.

	Instrument					
	1	2	3	4	6	Mean
Slope	0.24	0.66	0.39	0.34	0.54	0.38
Offset	0.04	0.01	0.01	0.00	0.01	0.01
Correlation Coefficient	0.14	0.86	0.72	0.74	0.36	0.56

Table 6. Linear regression slope, offset and correlation coefficient for observed vs. theoretical setup

THIS PAGE INTENTIONALLY LEFT BLANK

## VI. DISCUSSION

The  $H_{\text{rms}}$  values using (10) derived from the pressure sensors located up in the water column, in general, have a positive bias (Table 1) compared with the buried Paroscientific pressure sensors. The Bernoulli effect caused by water flowing past the pressure sensor orifices comes as an  $u^2$  term, which always gives a positive contribution. The Bernoulli effect acts to overestimate waves. Therefore, the buried pressure sensors were used to estimate radiation stress.

Setup/down observations obtained using buried Paroscientific pressure sensors during the Nearshore Canyon Experiment confirms the balance between cross-shore reduction in wave momentum and increase in mean surface elevation. The positive pressure gradient within the surfzone is a response to the decrease in radiation stress. Setup also increases with increasing wave heights, consistent with theory. Theoretical setup values obtained by integrating the cross-shore momentum equation numerically and using measured values of radiation stress as forcing underestimated measured values by about 40 percent in the mean. This is consistent with *Raubenheimer et al [2001]*, who found theory underestimated measurement by 40-90 percent in the inner surfzone in depths less than one meter.

The underestimated setup are based on using radiation stress calculated using linear theory transformation functions and measured velocities and or pressure measurements. The linear theory transformation functions account for momentum in the water column, but do not account for the momentum fluxes of the breaking waves between the trough and crest of the waves. These measurements suggest that a significant portion (60 percent) of the changes in momentum flux are associated with breaking wave processes between the trough and crest of the breaking wave.

Setdown was observed between Instrument 6 and 7, which is not predicted by the numerical solution of (1) using measured  $S_{xx}$  as forcing. Coarse resolution inherent in instrument spacing does not measure increases in radiation stress that relate to setdown when it occurs between instruments.

THIS PAGE INTENTIONALLY LEFT BLANK

## VII. CONCLUSIONS

Setup is defined as the superelevation of mean water surface within the surfzone and is caused by the reduction in wave momentum flux due to breaking waves with compensating positive pressure gradient. Data were acquired north of Scripps Canyon on a gently sloping section of beach, which was homogenous in along-shore morphology, during the Nearshore Canyon Experiment, 2004. Pressure sensors were deployed both above and below the bed. Wave heights and radiation stress (wave-induced momentum) were calculated using linear theory transfer functions. Wave heights measured using pressure sensors in the water column had a positive bias compared with the buried pressure sensors, which it is presumed due to the Bernoulli effect of flow past the sensor orifices. Predicted setup based on numerically solving the cross-momentum equation forced with the measured radiation stresses underestimates the observed in the inner surfzone setup by 40 percent in the mean. It is concluded that using pressure or velocity measurements with linear transfer functions to estimate wave momentum flux locally substantially underestimates the momentum flux that is occurring between the trough and crest of the breaking wave. This is consistent with previous studies.

THIS PAGE INTENTIONALLY LEFT BLANK

## FIGURES

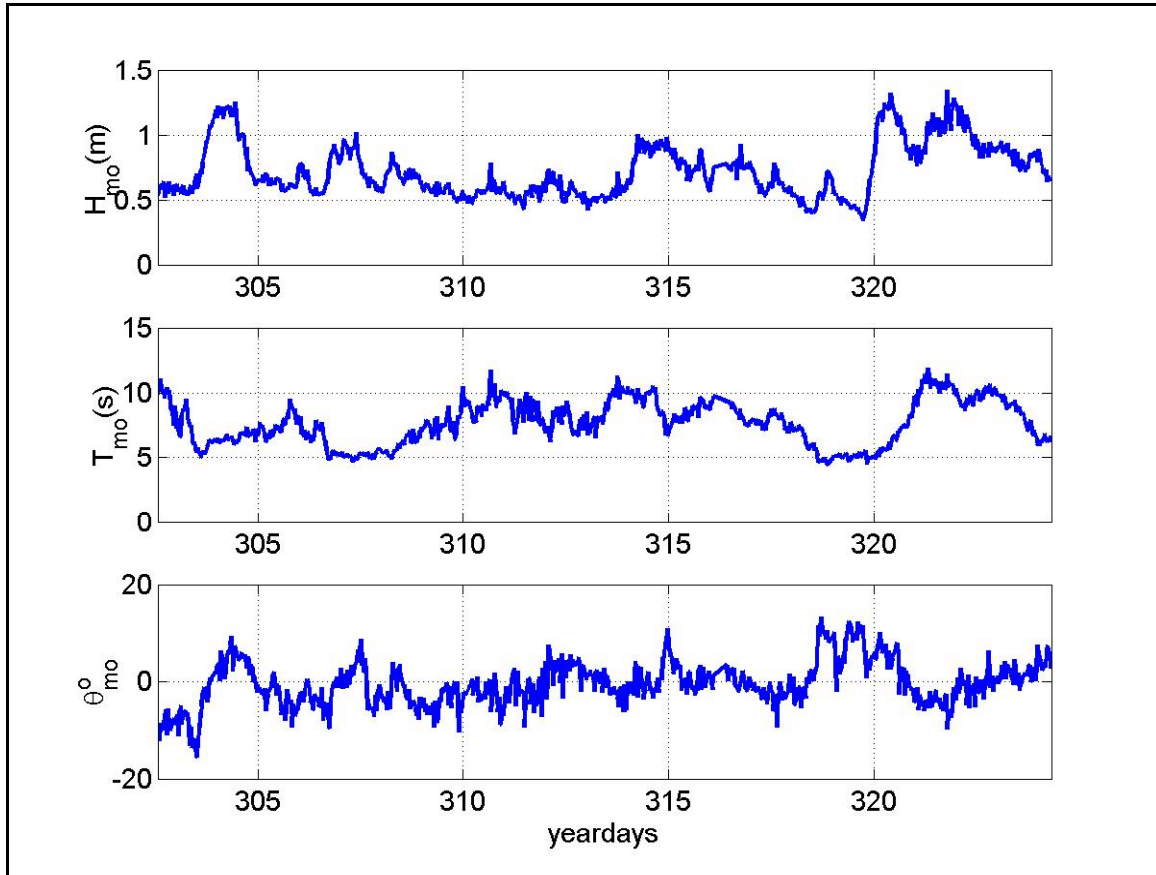


**Figure 1.** Observed wave height, period and direction over the course of the experiment.

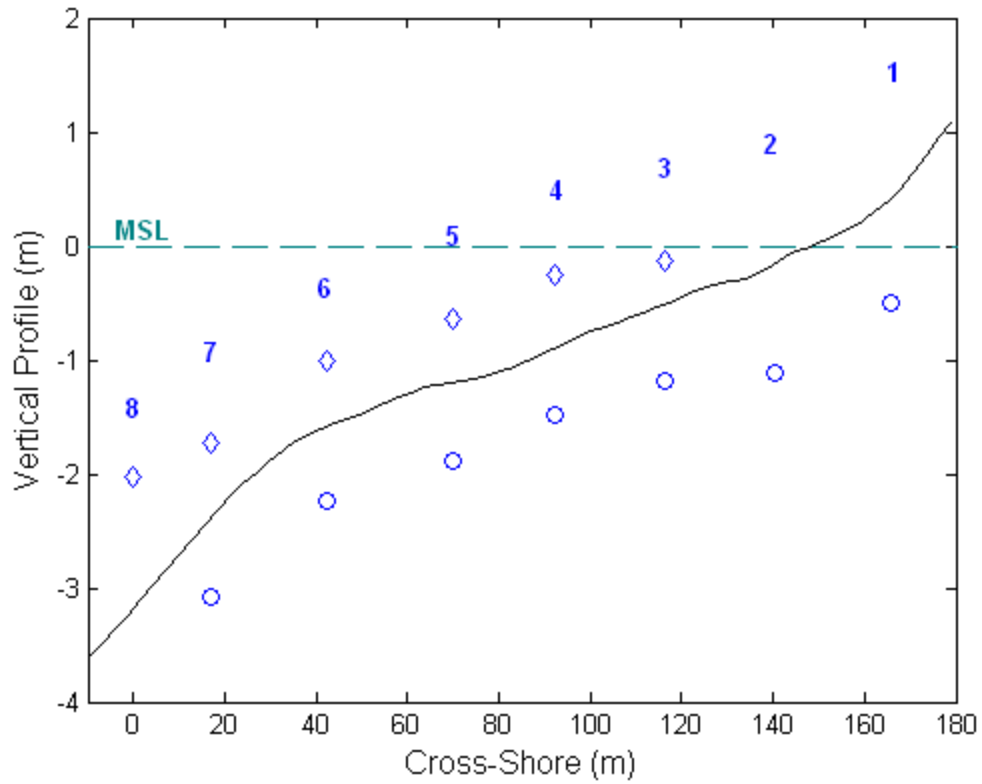


**Figure 2.** Location of Paroscientific and Kulite pressure transducers relative to the bed and mean sea level. Open circles beneath the profile represent Paroscientific sensors. Open diamonds signify Kulite sensors. Instruments are numbered from the closest onshore to the furthest off.

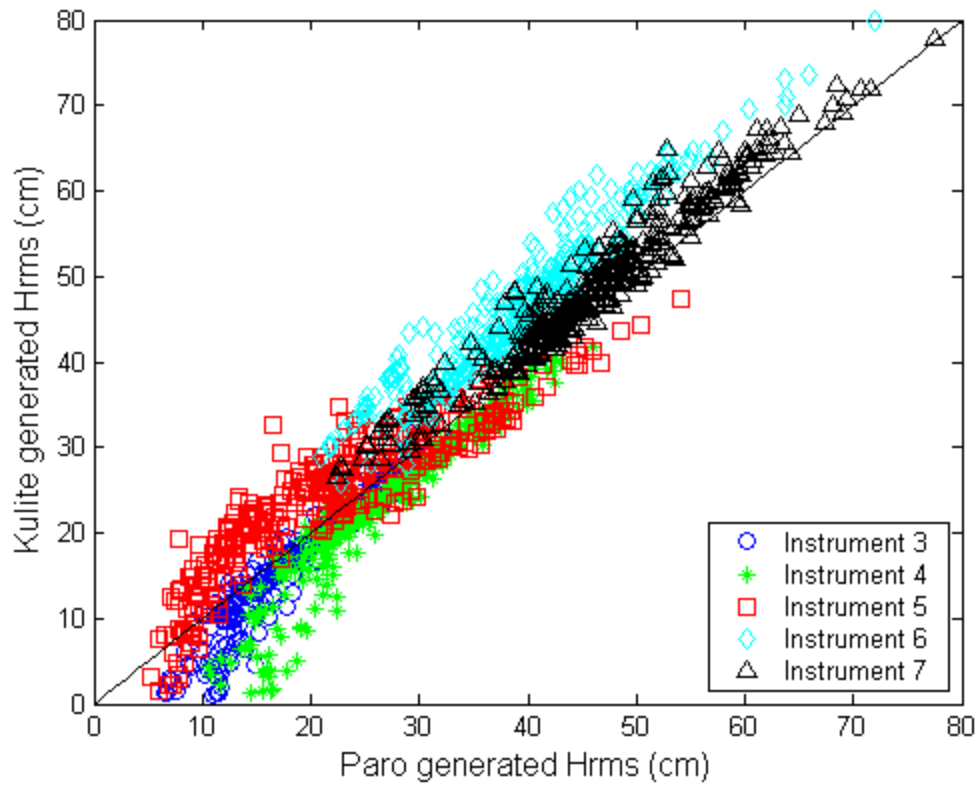


**Figure 3.** Wave heights (in cm) generated by colocated Paroscientific and Kulite pressure transducers.

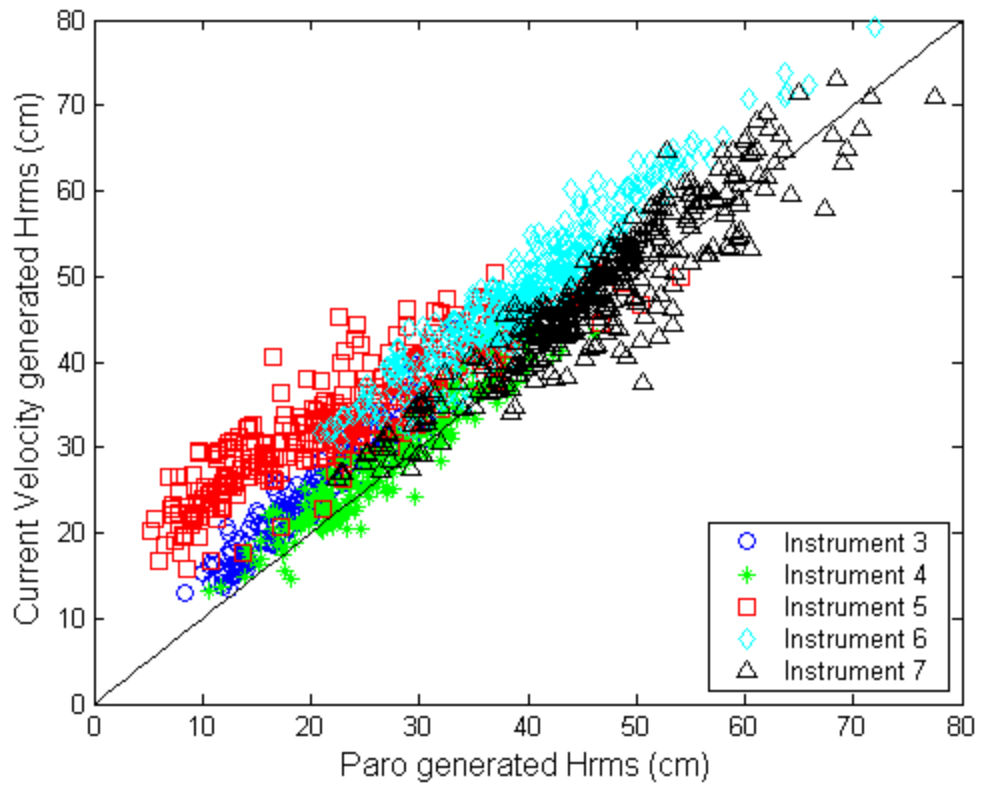


**Figure 4.** Wave heights (in cm) generated by colocated Paroscientific pressure transducer and Marsh McBirney electromagnetic current velocimeter.

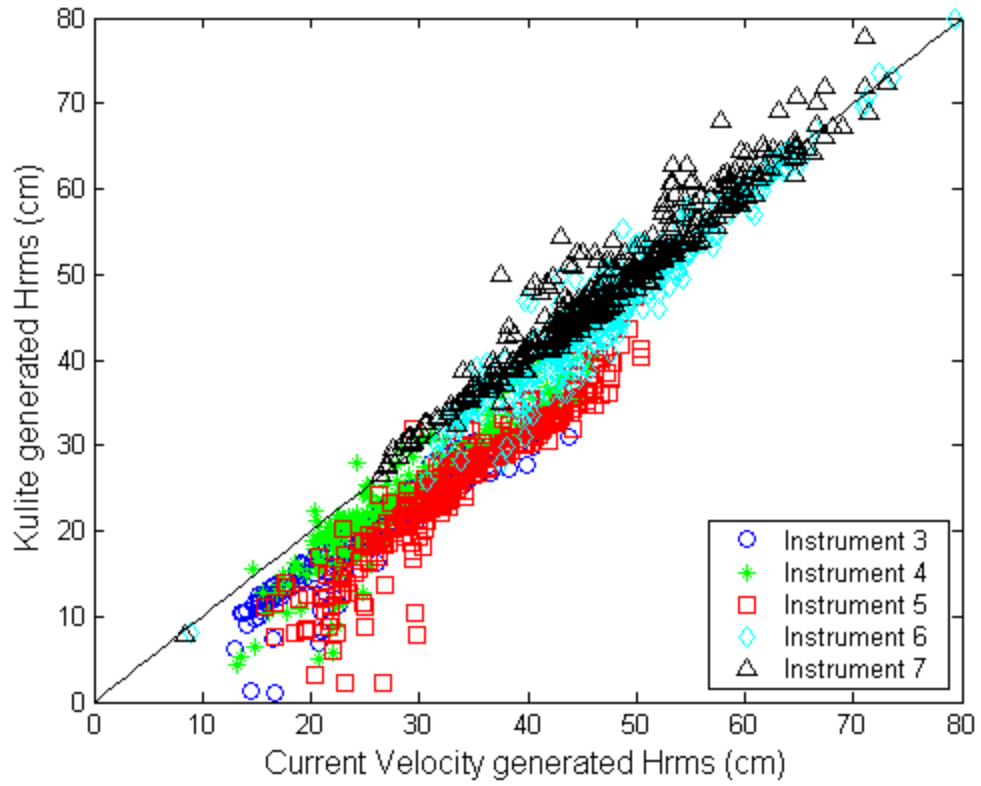


**Figure 5.** Wave heights (in cm) generated by colocated Marsh McBirney electromagnetic current velocimeter and Kulite pressure transducer.

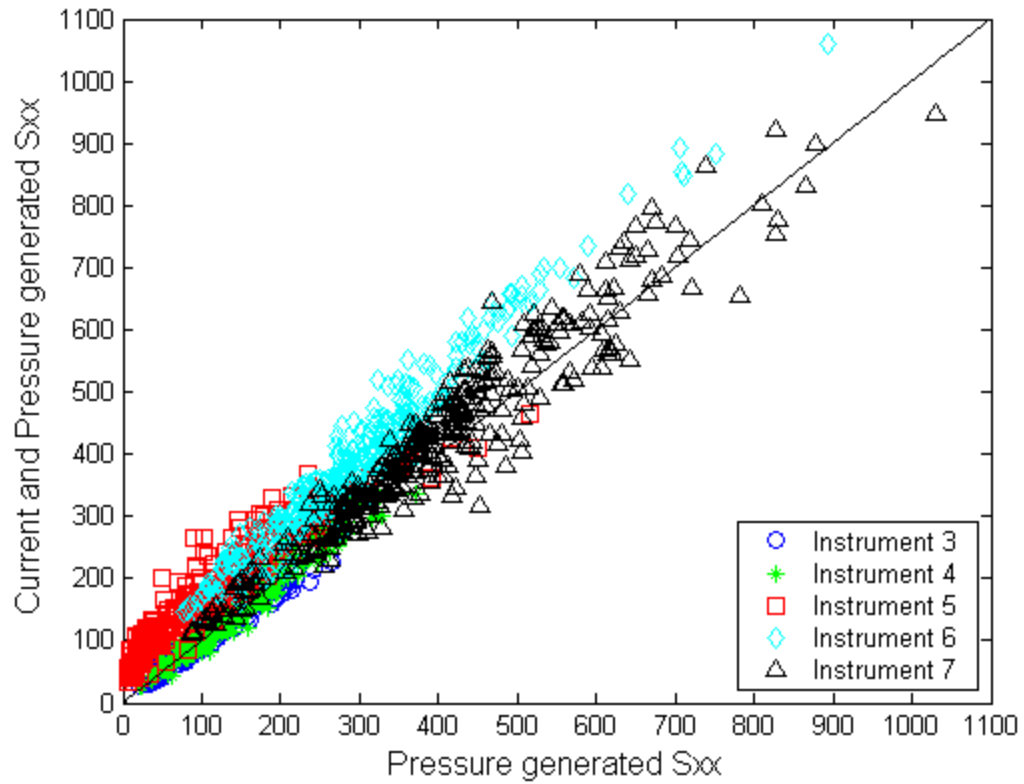


**Figure 6.** Radiation Stress generated by colocated Paroscientific pressure transducer and Marsh McBirney electromagnetic current velocimeter. Radiation stresses plotted on the abscissa were derived from pressure data alone. Radiation stresses plotted in the ordinate were derived from pressure and velocity data.

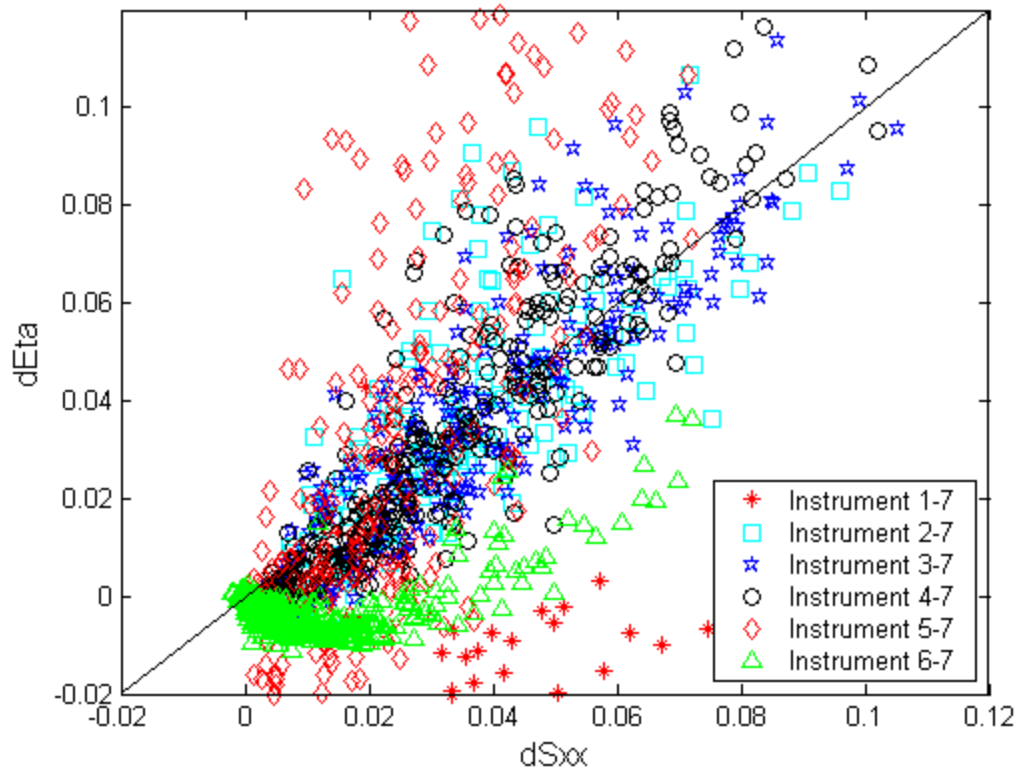


**Figure 7.** Calculated shoreward changes in radiation stress vs. surface elevation gradients between Instrument 7 and subsequent inshore instruments. The radiation stress gradient has been divided by  $-\rho g(h + \eta)$  for comparison.

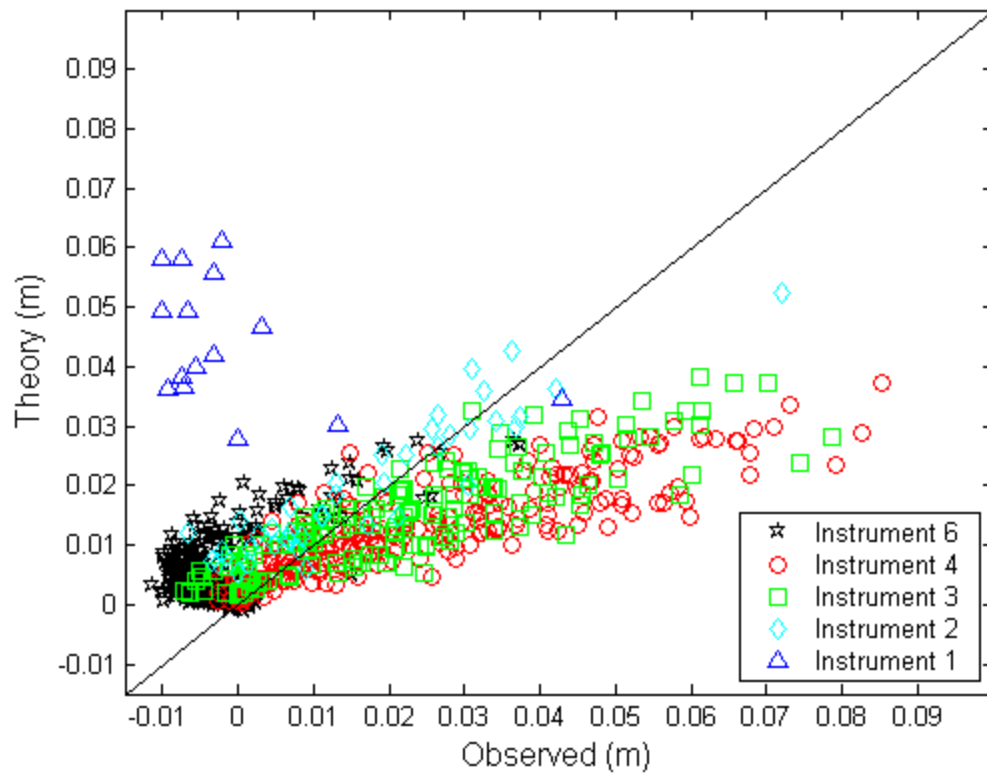


**Figure 8.** Observed superlevation of mean water level plotted against the theoretical setup. Instrument 5 is excluded.

## LIST OF REFERENCES

Battjes, J.A., “Computations of set-up, longshore currents, run-up overtopping due to wind-generated waves,” *Tech. Rep. 74-2*, Delft Univ. of Technol., Delft, Netherlands, 1974.

Battjes, J. A., and M. J. F. Stive, “Calibration and verification of a dissipation model for random breaking waves,” *J. Geophys. Res.*, 90, 9159-9167, 1985.

Battjes, J. A., and J. P. F. M. Janssen, “Energy loss and setup due to breaking of random waves,” *Proceedings from the 16<sup>th</sup> International Conference on Coastal Engineering*, ASCE, Hamburg, Germany, 1978.

Bowen, A. J., D. L. Inman, and V. P. Simmons, “Wave ‘set-down’ and set-up,” *J. Geophys. Res.*, 73, 2569-2577 1968.

Diegaard, R., P. Justesen, and J. Fredsøe, “Modeling of undertow by a one-equation turbulence model,” *Coastal Eng.*, 15, 431-458, 1991.

Fairchild, J. C., “Model study of wave setup induced by hurricane waves at Narrangsett Pier, Rhode Island,” *Bull. 12, U. S. Army Corps of Eng*, Washington D. C., 1958.

Guza, R. T., and E. B. Thornton, “Wave setup on a natural beach,” *J. Geophys. Res.*, 86, 4133-4137, 1981.

Haller, M. C., R. A. Dalrymple and I. A. Svendsen, “Experimental study of nearshore dynamics on a barred beach with rep channels,” *J. Geophys. Res.*, 107, 14-1–14-21, 2002.

King, B. A., M. W. L. Blackley, A. P. Carr, and P. J. Hardcastle, “Observations of wave-induced setup on a natural beach,” *J. Geophys. Res.*, 95, 22,289-22,297, 1990.

Lentz, S., and B. Raubenheimer, "Field observations of wave setup dynamics," *J. Geophys. Res.*, 104, 25,867-25,8875, 1999.

Longuet-Higgins, M. S., and R. W. Stewart, "Radiation stress and mass transport in gravity waves, with application to 'surf-beats,'" *J. Fluid Mech.*, 13, 481-504, 1962.

Longuet-Higgins, M. S., and R. W. Stewart, "A note on wave setup" *J. Mar. Res.*, 21, 4, 1963.

Nielsen, P., "Wave setup: A field study," *J. Geophys. Res.*, 93, 15,643-15,652, 1988.

Phillips, O. M., Dynamical conservation equations, in *The Dynamics of the Upper Ocean, Second Edition*, edited by G.K. Batchelor and J. W. Miles, pp 63-70, Cambridge University Press, Cambridge, England, 1977.

Raubenheimer, B., S. Elgar, and R. T. Guza, "Estimating wave heights from pressure measured in a sand bed," *J. Waterw. Port Coastal Ocean Eng.*, 124, 151-154, 1998.

Raubenheimer, B., R. T. Guza, and S. Elgar, "Field observations of wave-driven setdown and setup," *J. Geophys. Res.*, 106, 4629-4638, 2001.

Reniers, A. J. H. M., and J. A. Battjes, "A laboratory study of longshore currents over barred and non-barred beaches," *Coastal Eng.*, 30, 1-22, 1997.

Savage, R. P., "Model tests for hurricane protection project," *bulletin, Beach Erosion Board*, U. S. Cops Eng., Washington, D. C., 1957.

Saville, T., "Experimental determination of wave set-up," *Proceedings from the 2<sup>nd</sup> Tech. Conf. Hurricanes*, 242, 1961.

Schäffer, H. A., P. A. Madsen, and R. Deigaard, "A Boussinesq model for waves breaking in shallow water," *Coastal Eng.*, 20, 185-202, 1993.

Stive, M. J. F., and H. G. Wind, "A study of radiation stress and set-up in the nearshore region," *Coastal Eng.*, 6, 1-25, 1982.

Svendsen, I. A., "Wave heights and setup in the surf zone," *Coastal Eng.*, 8, 303-329, 1984.

THIS PAGE INTENTIONALLY LEFT BLANK

## INITIAL DISTRIBUTION

1. Defense Technical Information Center  
Fort Belvoir, Virginia
2. Dudley Knox Library  
Naval Postgraduate School  
Monterey, California
3. Dr. Mary Batteen  
Chairman  
Department of Oceanography  
Naval Postgraduate School  
Monterey, California
4. Dr. Ed Thornton  
Department of Oceanography  
Naval Postgraduate School  
Monterey, California
5. Dr. Timothy Stanton  
Department of Oceanography  
Naval Postgraduate School  
Monterey, California
6. CDR John Joseph, USN  
Program Officer  
Department of Oceanography  
Naval Postgraduate School  
Monterey, California
7. Dr. Jamie MacMahan  
Department of Oceanography  
Naval Postgraduate School  
Monterey, California
9. Commanding Officer  
Naval Oceanographic Office  
Stennis Space Center, Mississippi
8. LT Sean P. Yemm, USN  
Naval Oceanographic Office  
Stennis Space Center, Mississippi